ABSTRACT

Title of Document: QUENCHING LIMITS AND MATERIALS DEGRADATION OF HYDROGEN DIFFUSION FLAMES

Nicholas R. Morton, Master of Science in Fire Protection Engineering, 2007

Directed By: Assistant Professor, Peter B. Sunderland, Department of Fire Protection Engineering

This study examines the types of hydrogen leaks that can support combustion and the effects on various materials of long term hydrogen flame exposure. Experimental and analytical work is presented. Measurements included limits of quenching, blowoff, and piloted ignition for burners with diameters of 0.36 to 1.78 mm. A dimensionless crack parameter was identified to correlate the quenching limit measurements. Flow rates of 0.019 to 40 mg/s for hydrogen, 0.12 to 64 mg/s for methane, and 0.03 to 220 mg/s for propane were studied. Hydrogen quenching limits are found to have lower mass flowrates than those of methane and propane. Hydrogen blowoff mass flowrates are found to be higher than methane and propane. Materials degradation experiments were conducted on 1080 – 1090 carbon steel, 304 and 316 alloys of stainless steel, galvanized 1006 – 1008 carbon steel, aluminum alloy 1100, and silicon carbide fibers. Exposure to hydrogen flames is found to severely degrade aluminum alloy 1100. Noticeable corrosion is present on 304 and 316 stainless steel, galvanized 1006 – 1008 carbon steel. Silicon carbide fibers perform relatively similarly for hydrogen and methane flame exposure.

QUENCHING LIMITS AND MATERIALS DEGRADATION OF HYDROGEN DIFFUSION FLAMES.

By

Nicholas R. Morton

Thesis submitted to the Faculty of the Graduate School of the
University of Maryland, College Park, in partial fulfillment
of the requirements for the degree of
Master of Science
2008

Advisory Committee:
Assistant Professor Peter B. Sunderland, Chair
Associate Professor André Marshall
Associate Professor Frederick W. Mowrer

Dedication

To my Grandfather.

Acknowledgements

This work was supported by NIST (Grant 60NANB5D1209) under the technical management of J. Yang. I would like to express my gratitude to my advisor, Dr. Peter Sunderland, for his guidance, support, and encouragement. It has been my privilege.

I also thank my friend, Dr. Ezekoye at the University of Texas, for introducing me to the field of all things fire. His enthusiasm and guidance while I considered the pursuit of this degree were invaluable.

I thank my advisory committee, Dr. André Marshall and Dr. Frederick Mowrer, for their time and input.

The faculty of the Department of Fire Protection Engineering for the encouragement and support, and the friendly atmosphere that is the hallmark of this wonderful program, I cannot thank you enough.

Special thanks to the staff of the FPE office, specifically Patricia Baker and Allison Spurrier, who willingly take care of the hardest part of this whole process, the paperwork.

I would also like to thank my colleagues, for their assistance, reminders, and friendship. Specifically K.B. Lim, Vivien Lecoustre, and Chris Moran, were instrumental in the completion of this work.

I especially thank the Fire Protection community back home in Texas for insisting I needed this degree, my family and friends who supported my decision, and my nieces and nephews, for allowing me to go so far, for so long.

Table of Contents

List of Tables

List of Figures

Nomenclature

a	Dimensionless fuel-specific empirical constant
CP	Dimensionless crack parameter
d	Burner inside diameter
D_0	Mean diffusion coefficient
h	Standoff distance
HRR	Heat generated by the flame
L_b	Burner length
L_d	Flame standoff distance
L_f	Diffusion flame length
L_q	Quenching distance
M_{fuel}	Gas jet mass flowrate
Q_f	Volumetric fuel flowrate
Q_{wall}	Heat transferred to an area
Re	Reynolds number
u_0	Average fuel velocity in the burner
$Y_{F,stoic}$	Stoichiometric fuel mass fraction
Δp	Pressure drop across the burner
ρ	Fuel density
μ	Fuel dynamic viscosity

Chapter 1: Introduction

There is a need and a desire for alternative fuel and energy technologies in the near future [1]. Hydrogen is attractive because of the clean nature of its combustion processes, as well as the potential for a clean and renewable hydrogen source. The use of hydrogen lacks the level of investigation and refinement of more common fuels like methane and propane. There are many unknowns related to widespread hydrogen use. This study aims to determine some of the unknown risks, and present them in comparison to more widely used fuels such as propane and methane.

Concerns about the emissions of greenhouse gases and dependence on imported oil and natural gas have led to extensive consideration of hydrogen as a major fuel carrier. Hydrogen presents several unusual fire hazards, including high leak propensity, ease of ignition, and invisible flames. This research concerns experiments and analysis to identify which hydrogen leaks could support flames.

A small leak in a hydrogen system could ignite easily, support a flame that is difficult to detect, and degrade containment materials to the point of a catastrophic failure. An investigation into the effects of exposure to hydrogen at flame temperatures on representative materials is also presented.

Aspects of this work have been presented in Morton et al. [2, 3, 4, 5]. This work represents a more comprehensive discussion of these topics than is presented in Morton et al [2, 3, 4, 5].

1.1 Basics of Hydrogen

Hydrogen as a gaseous fuel exists in a diatomic state. As a fuel it possesses many desirable characteristics. It burns very cleanly; the simple global reaction with air is:

$$H_2 + 0.5\,(O_2 + 3.76N_2) \rightarrow H_2O + 1.88N_2 \qquad (1.1)$$

There is no CO_2 produced, which makes hydrogen a potential source of chemical energy that would reduce the emissions of this greenhouse gas [1,6]. The only products of combustion are water vapor and excess nitrogen.

Gaseous hydrogen has several properties which affect the nature of hydrogen gas combustion. The absence of carbon eliminates the primary source of heat radiation and visible light emission from standard hydrocarbon flames [7]. The result of this is a flame that is nearly invisible to the naked eye, and also difficult to sense via radiant heat output. The reaction zone is still very hot; the adiabatic flame temperature in air is as high as 2400 K [8].

1.2 Sources of Hydrogen

Hydrogen gas is produced in a variety of processes. Most hydrogen used commercially in the United States derives from fossil fuels [9]. The refinement of other hydrocarbons like acetylene and gasoline produce hydrogen gas as a byproduct. It is also manufactured directly from oil and natural gas specifically to produce hydrogen gas [10]. Anaerobic consumption of biomass such as wastewater sludge or livestock waste can be used to create hydrogen gas [9]. Hydrogen can also be derived from water using electrolysis. This process requires electricity, so the use of solar,

wind, and nuclear technology to produce electricity is often associated with the hydrogen economy. Nuclear processes can also create hydrogen by other means, without producing any additional byproducts outside of those produced through the normal operation of the reactor [11].

1.3 Hydrogen Safety

The properties of hydrogen that make it attractive, like a lack of carbon, and favorable ignition and flame stability characteristics, also create certain unique risks to the experimentalist; these risks are described here.

Methane and propane exhibit many of the characteristics of most other hydrocarbon fuels. They burn with a bright orange or yellow flame. Their flames radiate significant quantities of heat. Detection of a methane or propane flame during an experiment is therefore trivial. Hydrogen is very different however. Small hydrogen flames at the limit of quenching were not visible even in the darkened lab. Alternative methods were therefore devised to establish the existence or extinction of a hydrogen flame. The three methods used most often during the experiments were:

- Hot Plume Check: The investigator holds a hand over the burner to check for heat from the plume. A sensation of no heat does not necessarily mean no flame, but presence of heat is a very good indicator that a flame is present.
- Thin, Dry Paper Check: The investigator holds the corner of a thin dry piece of paper near the burner. If a flame is present the corner will char or ignite. A smoldering paper may also be used, with the added heat from the hydrogen flame resulting in a “flare up” event.

- Increase Flow Check: The investigator follows the procedure of reducing the flow until the flame quenches, then checks to make sure the flame quenched by increasing the flow again until a larger, visible hydrogen flame is present. If no flame exists at the higher flow, then quench was achieved.

These methods are necessary for all of the hydrogen experiments, as the initial flame in any experiment should always be somewhat small. For example, in the blowoff experiments, the initial flowrate for hydrogen is set to create a flame approximately 3 cm in height. This height is still not necessarily visible even in the darkened lab, so it is necessary to confirm ignition before attempting blowoff.

The automatic detection of hydrogen gas leaks and flames is a rare enough application that such detection is very expensive [12]. Therefore it is imperative that the person(s) using the apparatus are trained in the hazards associated with working with hydrogen. The safeguards employed during the course of this experiment included:

- Use only a limited supply of hydrogen, so failures in containment will still result in a relatively small release of hydrogen.
- Use only in a well-ventilated area, so small leaks will not result in a flammable or explosive accumulation of hydrogen.
- Utilize visible notifications of the presence of invisible flames, notifying laboratory personnel that the area around the apparatus could contain a flame even if there was no sensible light, heat, or sound.

- Adhere to rigorous experimental procedures to maintain the integrity of the apparatus.

1.4 Literature Review

Lovins [10] discusses the advantages of hydrogen as well as one method of introducing hydrogen as a common transportation fuel. Hydrogen is compared to natural gas and gasoline in terms of energy density, weight, volume, and cost. Lovins concludes that the current technology is sufficient to begin using hydrogen as a primary fuel immediately. Lovins also states "If all current global production of industrial hydrogen [were] fed into light vehicles…it would displace two-thirds of today's entire worldwide consumption of gasoline."

Bossel and Eliasson [13] conclude that hydrogen is too inefficient for widespread use. They discuss the high cost of manufacturing and transporting hydrogen. The high energy requirements of producing hydrogen from non-fossil fuel sources makes hydrogen too costly to be practical. Deriving hydrogen from fossil fuels is deemed worse for the environment, because "thermal losses limit the efficiency of hydrogen production…consequently, more CO_2 is released…than by direct use of the hydrocarbon precursors."

A Department of Energy report [14] found that hydrogen containment was the chief safety concern associated with using hydrogen as a transportation fuel. This report documents several catastrophic hydrogen fires. Hydrogen leaks can develop in pressure vessels, piping, seals, valves, pressure regulators, and pressure relief devices.

Khan et al. [15] discuss the effect of raised temperatures on carbon fabric/epoxy composites, a material that might be found in hydrogen containment

vessels [16]. The fatigue life was found to decrease at increasing temperatures, the decrease resulting from observed thermal degradation effects at temperatures around and exceeding 150 ˚C.

Pehr [17] discusses many of the aspects of hydrogen containment that must be considered before any allowance for a flame or flame effects is made. Pehr also highlights the need for specific investigations into the ramifications of using hydrogen as an energy carrier. Existing regulations regarding pressure vessels and gas plants may be inadequate, determination of their effectiveness can only be achieved through an open fact-finding investigation [17].

Utgikar and Thiesen [18] discuss the general safety of hydrogen fuel tanks, establishing two interesting ideas. The first is that no structural alloy is immune to hydrogen attack [18]. The reduction of material strength over time due to ambient condition exposure to hydrogen, and the need to account for this in the design of applications, has been shown [19,20]. The second is that hydrogen leaking from a high pressure tank into the ambient atmosphere will experience an increase in temperature between 25 and 33 ˚C [18]. The increase in temperature exacerbates the problems of hydrogen's innate low ignition energy.

Research in hydrogen combustion has increased recently, but no study to date has characterized the types of hydrogen leaks that can support a flame. Absent such information, it may be difficult for the designers of a hydrogen system to perform a cost-benefit analysis of protection against leaks.

Research has been done in quantifying leak flow rates, comparing hydrogen to methane and propane. Swain and Swain [21] modeled and measured leak rates for

diffusion, laminar, and turbulent flow regimes. They found that combustible mixtures in an enclosed space resulted more quickly for propane and hydrogen leaks than for methane leaks. However, their supply pressures were the same for all fuels and thus did not reflect plans for hydrogen systems in vehicles with pressures of up to 700 bar.

Measurements of propane quenching and blowoff flowrates were made by Matta et al. [22]. Matta et al. state that "fuel flow rates for which the predicted flame length is smaller than the measured standoff distance cannot sustain a flame." A hypothesis that is validated by the experimental results included in [22]. Matta et al. observe that "the flow rate at quenching is practically independent of the tube diameter." Matta et al. also provides a rationale for the prediction of blowoff, suggesting that "blowoff occurs when the predicted flow velocities in all flammable regions of the flame are larger than the local flame speeds." Experimental results are provided to support this hypothesis, although predicted values for blowoff are based on an assumed laminar flame speed much lower than those found in the literature [22]. Lee et al. [23] find that the anchoring point of lifted turbulent flames has an observed velocity higher than the maximum laminar flame speed, if sufficient upstream (before the burning region) mixing is allowed.

Measurements of methane quenching velocity were made by Cheng et al. [24]. Cheng et al. also provides a rationale for predicting the quenching velocity using the standoff distance and flame length correlations from various sources: "quenching should take place when the flame length predicted is equal to the standoff distance."

Data for methane and propane is available, but hydrogen quenching and blowoff measurements have not been reported.

Vanquickenborne et al. [25] studies the causes of "blow-out" and concludes that "blow-out phenomenon clearly is not due to an extinction phenomenon" because "a flame can be obtained at different heights if the ignition is maintained permanently."

Seade et al. [26] discuss the liftoff of methane jet diffusion flames. Liftoff is the point where the flame detaches from the anchor point on the flame holder. The effect of diluting the fuel on liftoff velocity is discussed, and the conclusion is that "fuel jet liftoff velocity decreases when dilution concentration [in the fuel stream] is increased."

Peters and Williams [27] discuss the analytical modeling of liftoff characteristics and define an instantaneous scalar dissipation rate, but state that "calculation of [scalar dissipation rate] requires parameters that are not generally available."

Rizk and Lefebvre [28] find in their study of laminar flame speed influences on blowoff that "the dominant fuel property affecting flame stability is … [the] laminar flame speed." They also provide values for laminar flame speed for hydrogen, methane, and propane, that match values found in [29].

Conduction to the physical boundary of the flame region is the dominant mode of heat transfer for hydrogen-air combustion, a fact established by Bregeon et al. [7]. The physical limitations of hydrogen-boundary interactions are important to the study of ignition and extinction, both for risk analysis as well as efficient combustion reactor designs. Existing estimates of quenching distance refer to

premixed flame propagation of stoichiometric mixtures, and the geometry used in the experimentation varies [8,29].

Ezekoye discussed the influence of water vapor condensation during premixed flame quenching [30]. The implication is that the phase change process that occurs when a hot flame region containing water vapor impinges on a cold surface, results in different heat losses from the flame than what is measured in terms of heat flux from the wall. The difference is the energy involved in the phase change from gaseous to liquid water. For hydrogen combustion, where water vapor dominates the combustion products, and conduction to the physical flame boundaries dominates the heat transfer, as established by [7], this effect has a potentially greater impact. Specific comparative studies of hydrogen quenching are required.

One goal of this research is to determine the relative fire hazards of hydrogen compared to methane and propane under small leak conditions. The modeling and experimentation focus primarily on small burners and flames near the quenching limit. Additional experimentation involves the exposure of various alloys of steel, stainless steel, aluminum, and SiC to hydrogen and methane flames.

Thus motivated, the objectives of this work are to: (1) Measure limits of flaming (at quenching and blowoff) for hydrogen, methane, and propane issuing from circular burners of various sizes; (2) Derive a parameter to predict limits of quenching from fuel properties; and (3) Examine material degradation arising from hydrogen and methane diffusion flames.

Chapter 2: Phenomena

2.1 Quenching

Quench occurs when a mixture of fuel and air that is still within normal limits of flammability is extinguished. This usually occurs when the temperature of the mixture falls below the critical flame temperature (circa 1500 K) due to heat transfer to the surroundings. In the case studied here, the cause is heat transfer to a boundary wall. As shown in Figure 2.1, when the heat generated by the flame (*HRR*) is less than the heat lost to the boundary (Q_{wall}), quenching will eventually occur. Quenching distances have been measured for flames propagating through stoichiometric mixtures in tubes or between flat plates, but minimum fuel flowrates to sustain a flame on a surface are not readily available. Predictions of these fuel rates require a heat transfer model that focuses on highly localized boundary effects. Material properties are also required for such an analysis. Direct measurements of these flowrates are required to verify any predictions, but should also be useful for design applications.

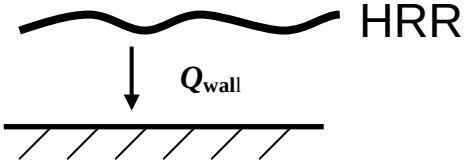

Figure 2.1: If the heat lost to the boundary (q'') exceeds the heat generated by the flame (q'''), quenching will occur.

2.2 Standoff Distance

The standoff distance of flames for various fuel types has been identified [21, 24] as independent of flame size, and constant for a given fuel and burner geometry. Other

studies of quenching predict the value by equating this standoff distance to flame length correlations. The idea is that the flammable mixture that would burn in that region must travel far enough away from the boundary to sustain itself. The flame length correlations do not capture this phenomena, and so their direct application combined with measurements of the standoff distance work well for predicting quenching. Figure 2.2 illustrates the standoff distance as it relates to flame length and quenching.

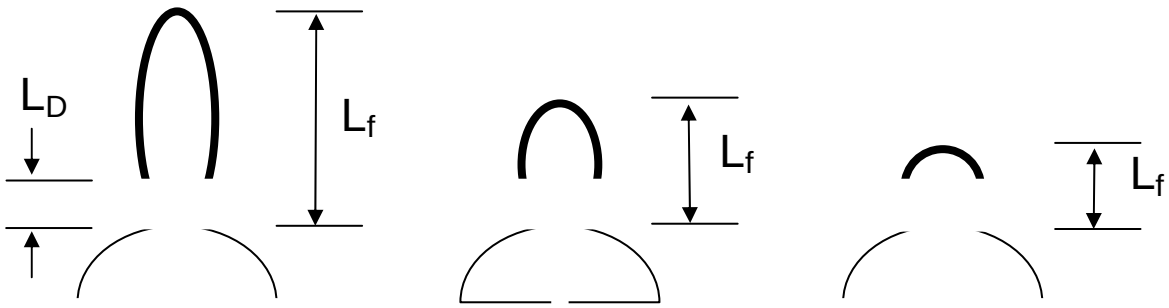

Figure 2.2: Standoff distance L_D as it relates to flame length L_f.

2.3 Blowoff

Blowoff occurs when the flammable mixtures of fuel and air all exceed the maximum laminar flame speed. A flame at low flow rates will start out like those shown in Figure 2.2. As the flow rate is increased, the anchoring points of the flame eventually achieve a mixture velocity equivalent to the laminar flame speed. As the flow rate continues to increase, these anchoring points will lift off of the burner, resulting in a lifted flame. Further increases in the flow rate can cause all regions of

the flame to exceed the laminar burning velocity, and the flame will blow off. This is shown in Figure 2.3.

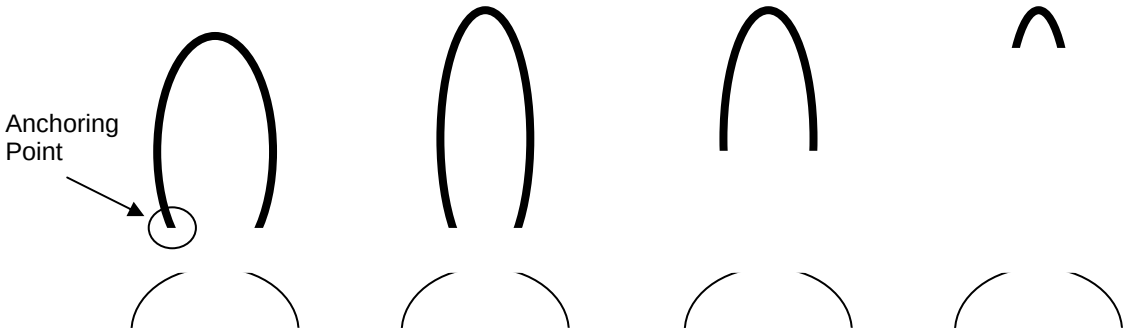

Figure 2.3: A diffusion flame will increase in size up to a maximum flame length. The anchoring points will then lift off of the burner, resulting in a lifted flame. As the flow rate continues to increase, the flame destabilizes and blows out.

Chapter 3: Quenching and Blowoff Limits

This chapter discusses the experiments performed during the course of this research. Descriptions of the phenomenon studied, the experimental apparatus used in the experiments, and the experimental procedures are included here.

The results of these efforts are provided in this chapter. The formulation of a parameter to predict the quenching limits based on fuel properties is discussed, and then compared with the experimental results obtained from the experiments described. The results of the quenching and blowoff experiments are provided, and a discussion of how these results compare with initial hypotheses is also provided.

3.1 Crack Parameter

The quenching limit is the minimum flowrate at which a diffusion flame can survive. Quenching arises from heat losses from conduction, radiation, and from losses of radicals to solid boundaries. The limit is affected by geometry, fuel, oxidizer, and surrounding materials. The quenching limit is the critical parameter for determining if a small fuel leak will be able to sustain a flame. For different materials, it can also be used to characterize the heat transfer from a flame region to the material.

Existing studies of quenching focus primarily on the premixed quenching distance, which is useful in combustion reactor design. It is unclear if the application of this quenching distance to diffusion flames that typically result from fuel leaks is justified. The premixed quenching distance is measured by the minimum diameter

tube that will allow a flame to propagate through a stoichiometric mixture. By measuring the quenching limit and comparing it to the premixed quenching distance, it should be possible to relate the two, clarifying the relationship between the fuel leak application and the quenching distance data.

A theoretical model was developed to predict flame quenching limits. This theory also yields a dimensionless crack parameter that indicates how close a given leak is to the quenching limit.

The starting point is this relationship for the stoichiometric length L_f of laminar gas jet diffusion flames on round burners:

$$L_f / d = a\, Re = a\, \rho\, u_0\, d / \mu\,, \tag{3.1}$$

where d is burner inside diameter, a is a dimensionless fuel-specific empirical constant, Re is Reynolds number, u_0 is the average fuel velocity in the burner, ρ is fuel density, and μ is fuel dynamic viscosity. The scaling of Eq. (3.1) arises from many theoretical and experimental studies, including Roper [31], Sunderland et al. [32] and references therein. Constant a here is assigned values determined by Sunderland et al. [32].

The base of an attached jet diffusion flame is quenched by the burner. Its standoff distance can be approximated as the quenching distance of a stoichiometric premixed flame. This distance is one half the diameter of the smallest tube a premixed flame can propagate through. Such quenching distances typically are reported as the minimum tube diameters through which a premixed flames can pass,

L_q. We assume here that a jet flame can be supported only if its stoichiometric length is greater than this quenching distance.

$$L_f \geq L_q / 2 \text{ to support a flame} \tag{3.2}$$

Values of L_q are taken from Kanury [29], reproduced in Table 3.3. When combined, Eqs. (3.1) and (3.2) predict the following gas jet mass flowrate, m_{fuel}, at the quenching limit:

$$m_{fuel} = \pi L_q \mu / (8 a) \tag{3.3}$$

Eq. (3.3) indicates that the mass flow rate at the quenching limit is a fuel property that is independent of burner diameter.

A crack parameter can now be derived. Assuming fully-developed laminar pipe flow in the burner,

$$u_0 = d^2 \Delta p / (32 \mu L_b) \tag{3.4}$$

where Δp is the pressure drop across the burner and L_b is the burner length.

Combining (3.1), (3.2) and (3.4) yields

$$CP = a \rho d^4 \Delta p / (16 \mu^2 L_b L_q) \geq 1 \text{ to support a flame,} \tag{3.5}$$

where CP is the dimensionless crack parameter.

Matta et al. [22] presents a theory to predict quenching based on the standoff distance of the flame and a prediction of flame length. The equation cited in Matta et al. [22] is reproduced here as (3.6):

$$L_f \approx [\, 3 / (8 * \pi) \,]* [\, Q_f / (D * Y_{F,stoic})] \tag{3.6}$$

where the volumetric flowrate Q_f that produces a flame length L_f equal to the measured standoff distance will be the quenching flowrate. D is the diameter of the burner, and $Y_{F,stoic}$ is the stoichiometric fuel mass fraction. This theory depends on an experimentally determined standoff distance: $h = L_{f,quench}$ [22]. The standoff distance is approximately constant for propane flows less than 2.5 cc/min.

Cheng et al. [24] also stipulates that the quenching condition may be predicted by equating the standoff distance to the flame length, using the correlation (3.7),

$$L_f = \{ Q_f / [\, 4 \pi D_O \ln(1 + 1 / S) \,] \} * (T_O / T_f)^{0.67} \tag{3.7}$$

where D_O is a mean diffusion coefficient, T_O is the oxidizer temperature, T_f is the flame temperature, and S is the molar stoichiometric oxidizer-fuel ratio. Q_f is equal to the volumetric flowrate at quenching when L_f is equal to the standoff distance. Cheng et al. [24] also observe that the quenching velocities follow a Re x d = constant curve. Values for the standoff distance are also experimentally determined for the results in [24], and assumed to be constant across burner diameters.

3.2 Experiments

Measurements were made of the quenching and blowoff limits of small-scale hydrogen, methane, and propane flames. Five burners of different diameters were used to measure the quenching limits. Flowrates were measured with calibrated rotameters. Diffusion flames were observed, at the near quench limit, and near blowoff limit.

3.2.1 Quenching Limit Experimental Setup and Procedure

For quenching limits, the burners are hemispherical stainless steel nozzles that can be found in many spray applications. At the apex of the hemisphere is a drilled hole. A schematic is shown in Figure 3.1.

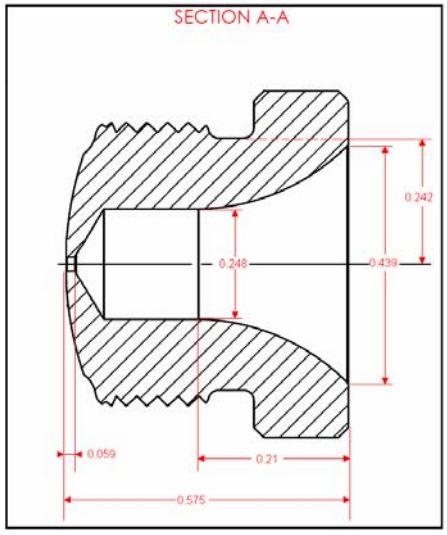

Figure 3.1: BEX burner schematic.

The burners were manufactured by BEX, the part numbers and corresponding effective diameters are summarized in Table 3.1. These burners were acquired directly from the manufacturer.

Table 3.1: BEX burner summary.

Burner Designation	Hole Diameter (mm)
WN14	0.356
WN28	0.711
WN33	0.838
WN55	1.397
WN70	1.778

The quenching limits were measured using a Gilmont® Instruments GF – 3060 shielded microflowmeter. Ranges of flows measured using this flowmeter were 0.015-0.030 mg/s of hydrogen, 0.10-0.12 mg/s of methane, and 0.02-0.05 mg/s of propane. This flowmeter was calibrated with air using a 10 cc Supelco Bubble Flow meter. Uncertainty of the flow rate measurements is estimated at ±5% per the manufacturer specifications.

The flow system was designed to provide a consistent flow of fuel to the burner port. A schematic of the flow system is shown in Fig. 3.2. The fuel source is high pressure bottled gaseous hydrogen and methane, and liquid bottled propane (A). Pressure regulators, (C) used to reduce the pressure to 2.75-3.45 bar. The regulators feed fuel into a needle valve (D). Downstream of this valve is a particulate filter (E) that ensures adequacy of the pressure relief valve. An emergency pressure relief valve (F), set to 7 bar, is just downstream of the filter (E), is used to prevent a failure of the bottle regulator from exceeding the pressure limits of any other components. Farther downstream is another needle valve (G), located to allow the downstream pressure regulator (H) to be isolated from the rest of the system. This helps diagnose leaks and provides an additional way to shut off the fuel closer to the rest of the experiments. The downstream pressure regulator (H) allows further manipulation of the fuel flow. This regulator is used in conjunction with a fine needle valve (I) to set fuel flowrates.

The fine needle valve (I) is the primary means of adjusting the fuel flow in all of the experiments. Downstream of this metering valve is the rotameter (J) and then the BEX burners (K).

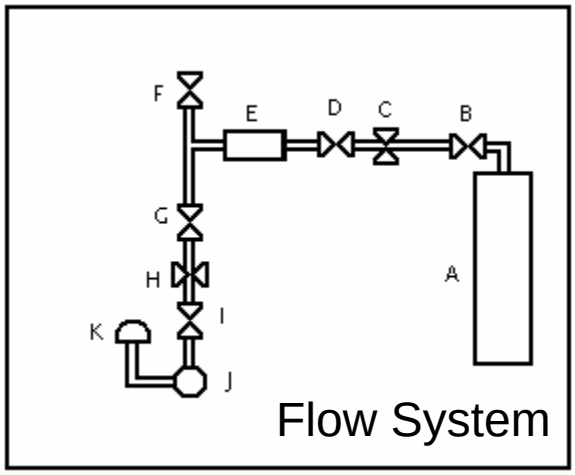

Figure 3.2: Flow system schematic. Gas cylinder A, Needle Valve B, Regulator C, Needle Valve D, Filter E, Relief Valve F, Needle Valve G, Regulator H, Fine Metering Needle Valve I, Rotameter J, BEX burner K.

Each fuel was passed through the burner and ignited, creating a flame approximately 5 mm long. The fuel flow was then reduced quickly using the fine needle valve until the flame extinguished. This was done several times for each burner and each fuel. The flames were small enough, and the experiment was done quickly enough, that there was no noticeable increase in the temperature of the burner. Temperature difference was determined qualitatively. If the burner was too hot to touch, that data point was considered to be potentially influenced by preheating of the fuel and air as it passed through and around the burner, and the data point was discarded.

3.2.2 Blowoff Experimental Modifications

The fuel flowrate at blowoff flow of each fuel for each burner was measured. Blowoff is the condition where the flame lifts off the burner and extinguishes. Blowoff occurs when the gas velocity in the entire flame region exceeds the laminar flame speed [22,25,28]. The setup for blowoff tests was similar to that for the quenching experiments. The differences are explained in this section.

The blowoff regime for each fuel varied sufficiently that multiple rotameters were required to cover the range of flowrates. There were four rotameters used during this stage of the experiments. They are summarized in Table 3.2.

Table 3.2: Rotameter model information and measurement ranges.

Flowmeter Model	Air flow range (m^3/min)	H_2 (mg/s)	CH_4 (mg/s)	C_3H_8 (mg/s)
Omega FL - 2001 - NV	4.72 – 47.2	0.25 - 2.67	0.71 - 7.55	1.17 - 12.5
ABB 10A6133AB1E	14.2 – 141.6	0.48 - 5.34	1.36 - 15.11	2.26 - 25.06
Omega FL - 2034 - NV	188.8 – 1887.7	15.1 - 91.4	42.69 - 258.51	70.79 - 428.7

The high flowrates required for blowoff also required the metering valve to be replaced with a larger valve. The large diameter burners for hydrogen required flowrates that exceeded the capabilities of the flow system, resulting in an inability to measure the hydrogen blowoff limits for the 1.397 mm and 1.778 mm diameter burners.

The blowoff experiments began by igniting a flow of fuel, and then increasing the flow rate until the flame lifts off and is eventually extinguished. Hearing protection was required during these tests, especially for hydrogen. Prior to blowoff, flames will lift off of the burners. Turbulent flames were sometimes observed and

these tended to be shorter than the diffusion flames immediately after transition to turbulence occurs, changing from a 0.3-0.4 m laminar flame to a 0.2 m turbulent flame, but as the flow increases the flame length can still be in excess of 0.5 m. Turbulent flames were observed during the experiments at greater than 1 m in height before blowoff could be achieved.

3.3 Quenching and Blowoff Results

The results of the quenching and blowoff are presented here as massflows, m_{fuel}, vs. burner diameter in Figs. 3.3, 3.4, and 3.5 for hydrogen, methane, and propane, respectively. The results are compared qualitatively to each other.

The results are also presented as fuel velocities, u_0, here in Figs. 3.6, 3.7, and 3.8 for hydrogen, methane and propane respectively. These figures (3.3-3.8) also include the predictions of quenching from our laminar pipe flow theory, described in Section 3.1, as well as data on propane and methane from Matta et al. [22] and Cheng et al. [24].

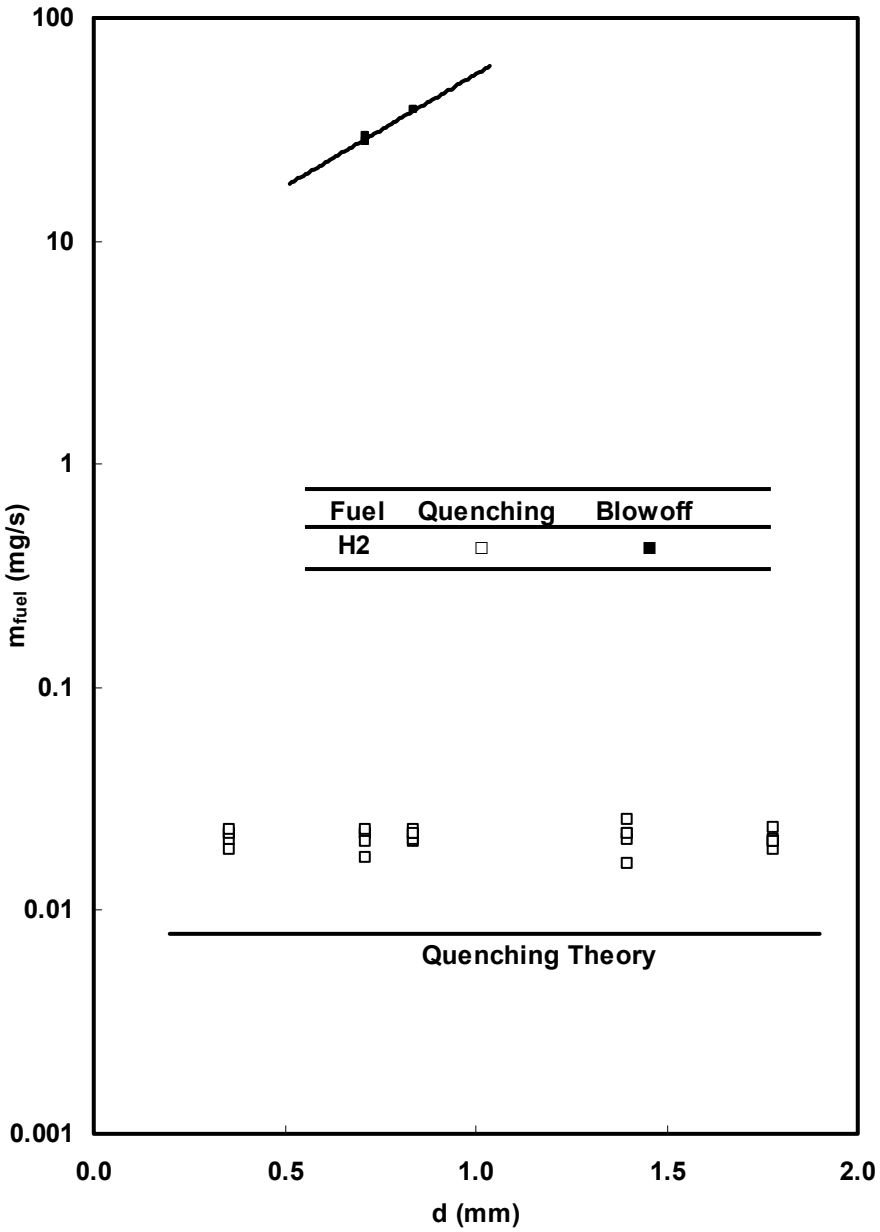

Figure 3.3: Hydrogen quenching and blowoff mass flowrate limits vs. burner diameter. The Quenching Theory line represents the prediction for quenching from the application of Eq. 3.5. The line through the blowoff points is a curve-fit highlighting the trend observed for that phenomenon.

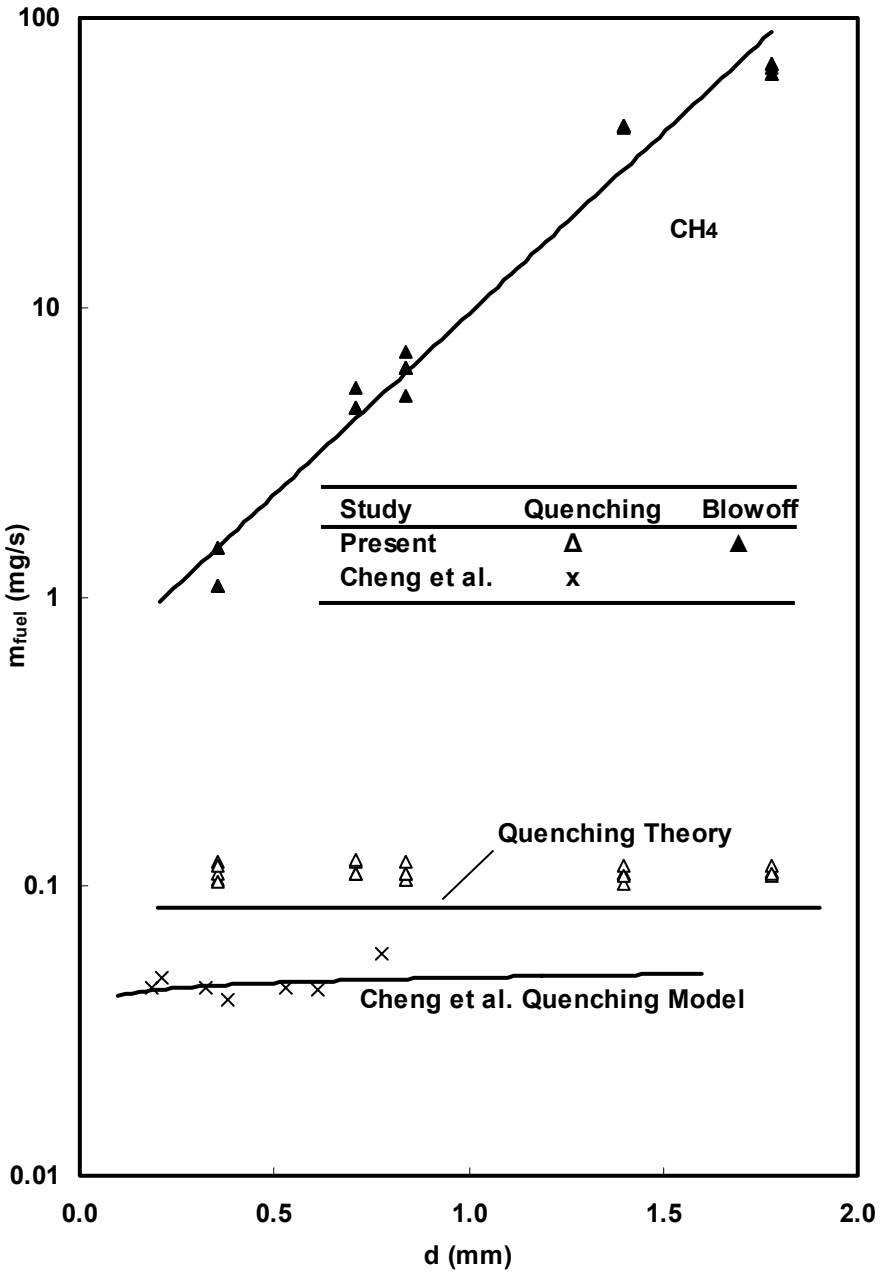

Figure 3.4: Methane quenching and blowoff shown as mass flowrate vs. burner diameter. The quenching theory line represents the prediction for quenching from the application of Eq. 3.5. The line through the blowoff points is a least-squares fit. Quenching data and model prediction for methane from Cheng [24] are also shown.

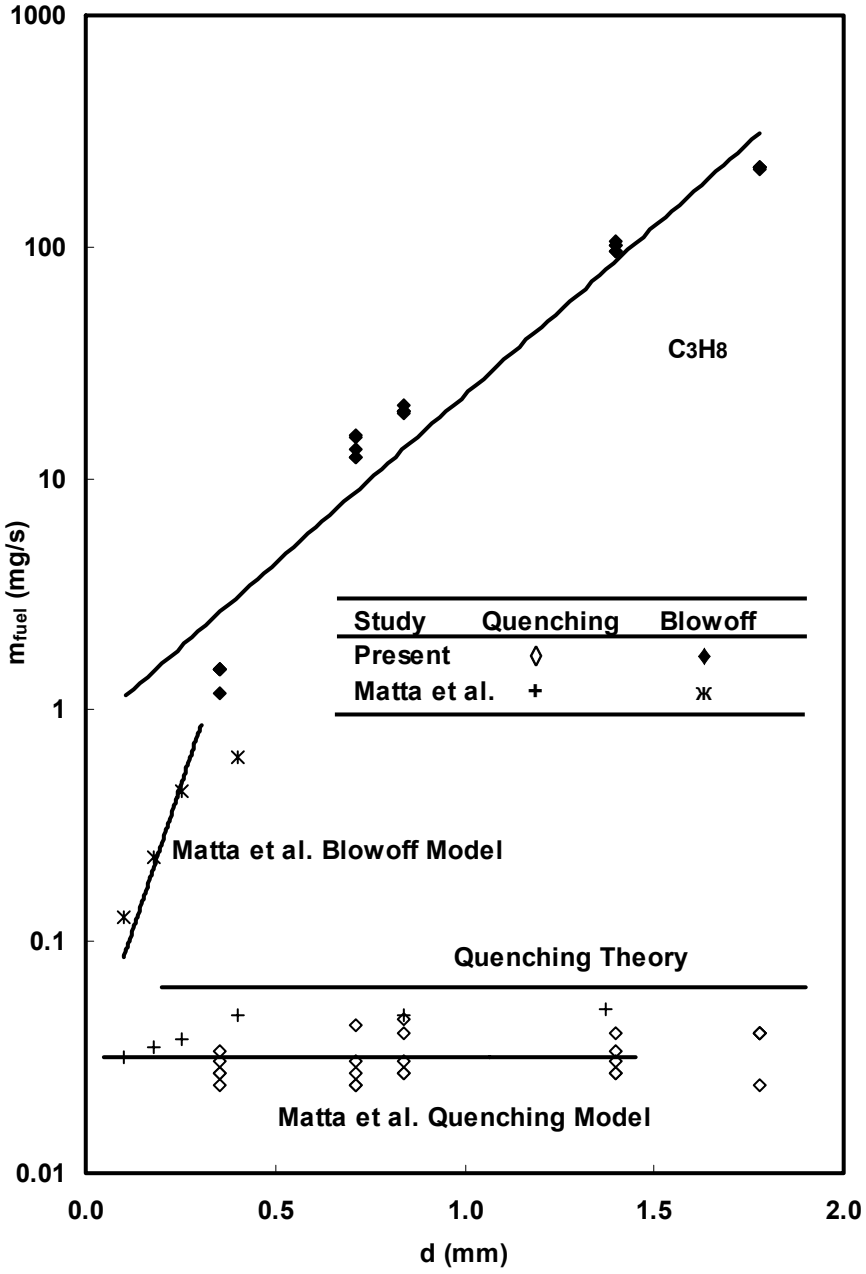

Figure 3.5: Propane quenching and blowoff limits shown as mass flowrate vs. burner diameter. The Quenching Theory line represents the prediction for quenching from the application of Eq. 3.5. The line through the blowoff points is a curve-fit highlighting the trend observed for that phenomenon. Quenching data and model prediction, as well as blowoff data and model prediction for methane from Matta et al. [22] are also shown.

From Fig. 3.3-3.5 hydrogen requires the smallest flowrate at quenching, which is expected from Eq. (3.3). Propane requires slightly higher mass flow rates, and methane requires the highest.

A crack parameter based on a laminar pipe flow comparison is also shown on the plots. While the theory seems to capture the curves and trends of the quenching experiments, the actual values of this simple model do not agree very well. The Matta et al. [22] quenching model based on standoff distance instead of quenching distance generally agrees with these quenching measurements for propane. The Cheng et al. [24] model, derived in the same way, does not agree as well with our methane quenching measurements.

Of particular note is that the crack parameter dependence on burner diameter drops out of the equation when it is solved for a massflow. This aspect of the theory is also demonstrated by the experiments. For a given fuel, there exists a critical mass flowrate, below which sustained ignition is not possible, independent of burner diameter. This was noted and confirmed for other fuels [22,24,27], and is found to be consistent with hydrogen. The implication is that if we can determine the flowrate through a leak, then we know whether that leak will be flammable or not. Table 3.3 presents selected fuel properties and summarizes the minimum flowrate necessary to support a flame for each fuel, calculated as the average of the quenching limit from all of the experiments.

Table 3.3: Selected Fuel Properties.

Fuel	a	L_q [m]	S_L [cm/s]	μ	Quenching Flowrate (mg/s)
H2	0.236	0.51	291	8.76E-03	0.022
CH4	0.136	2.3	37.3	1.09E-02	0.101
C3H8	0.108	1.78	42.9	7.95E-03	0.056

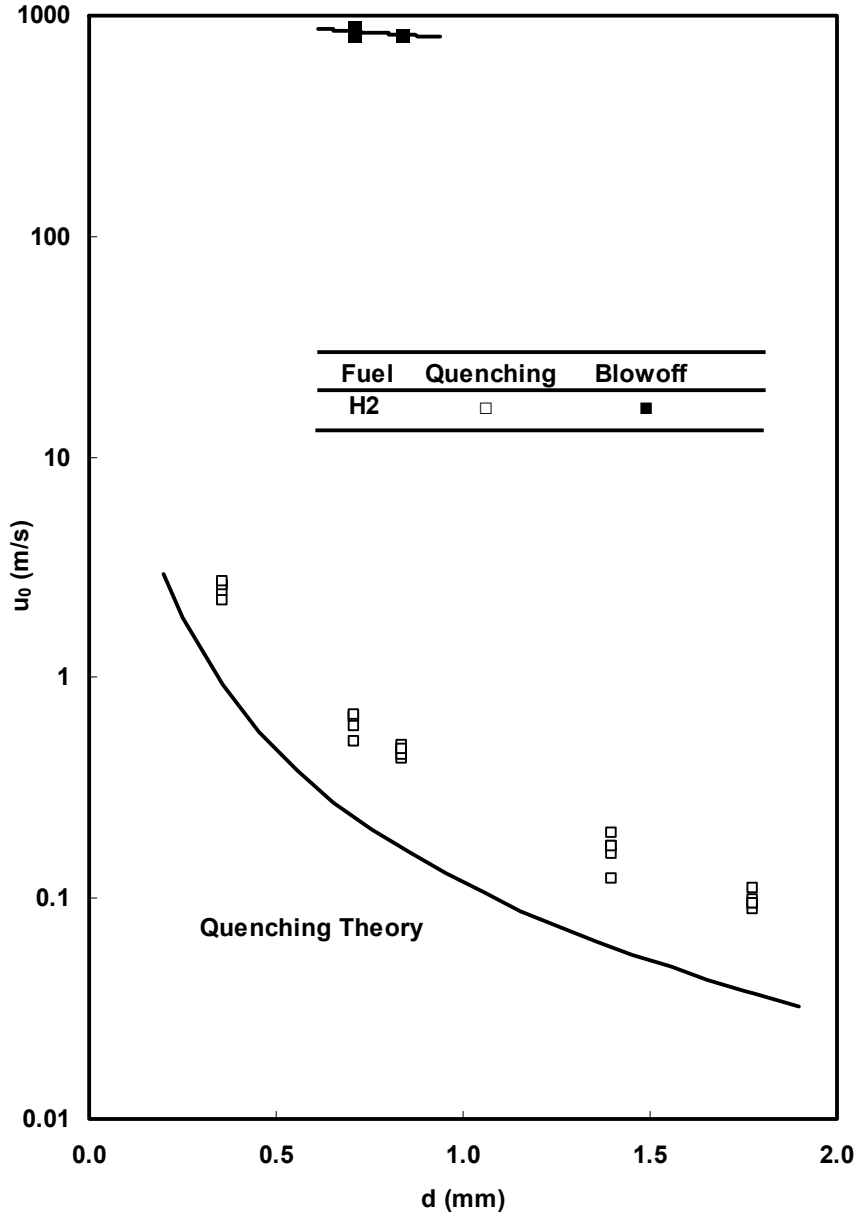

Figure 3.6: Hydrogen quenching and blowoff velocity limits vs. burner diameter. The Quenching Theory line represents the prediction for quenching from the application of Eq. 3.5.

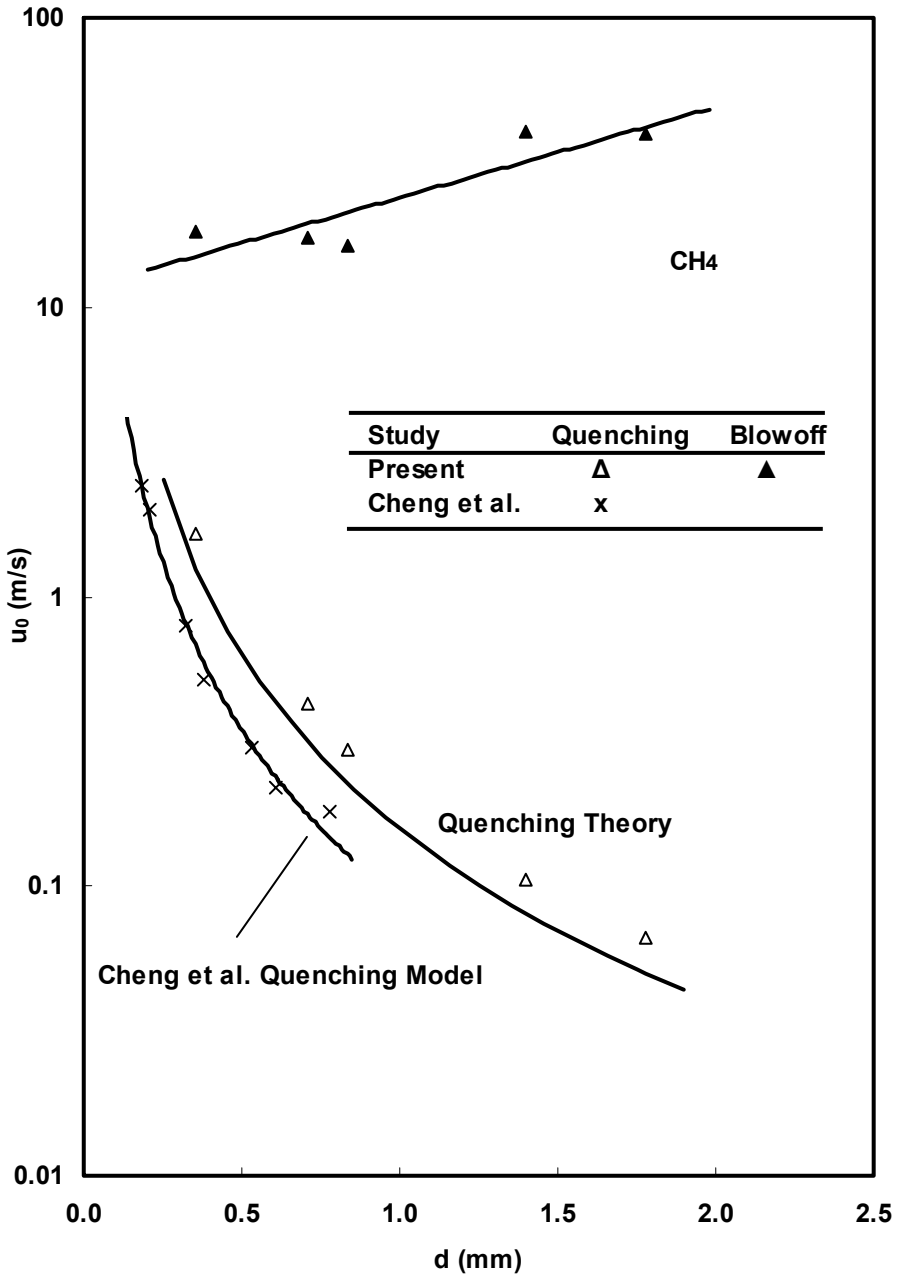

Figure 3.7: Methane quenching and blowoff shown as fuel velocity "u_0" vs. burner diameter. The Quenching Theory line represents the prediction for quenching from the application of Eq. 3.5. Quenching and blowoff data for methane is shown, along with theory and results from Cheng et al. [24].

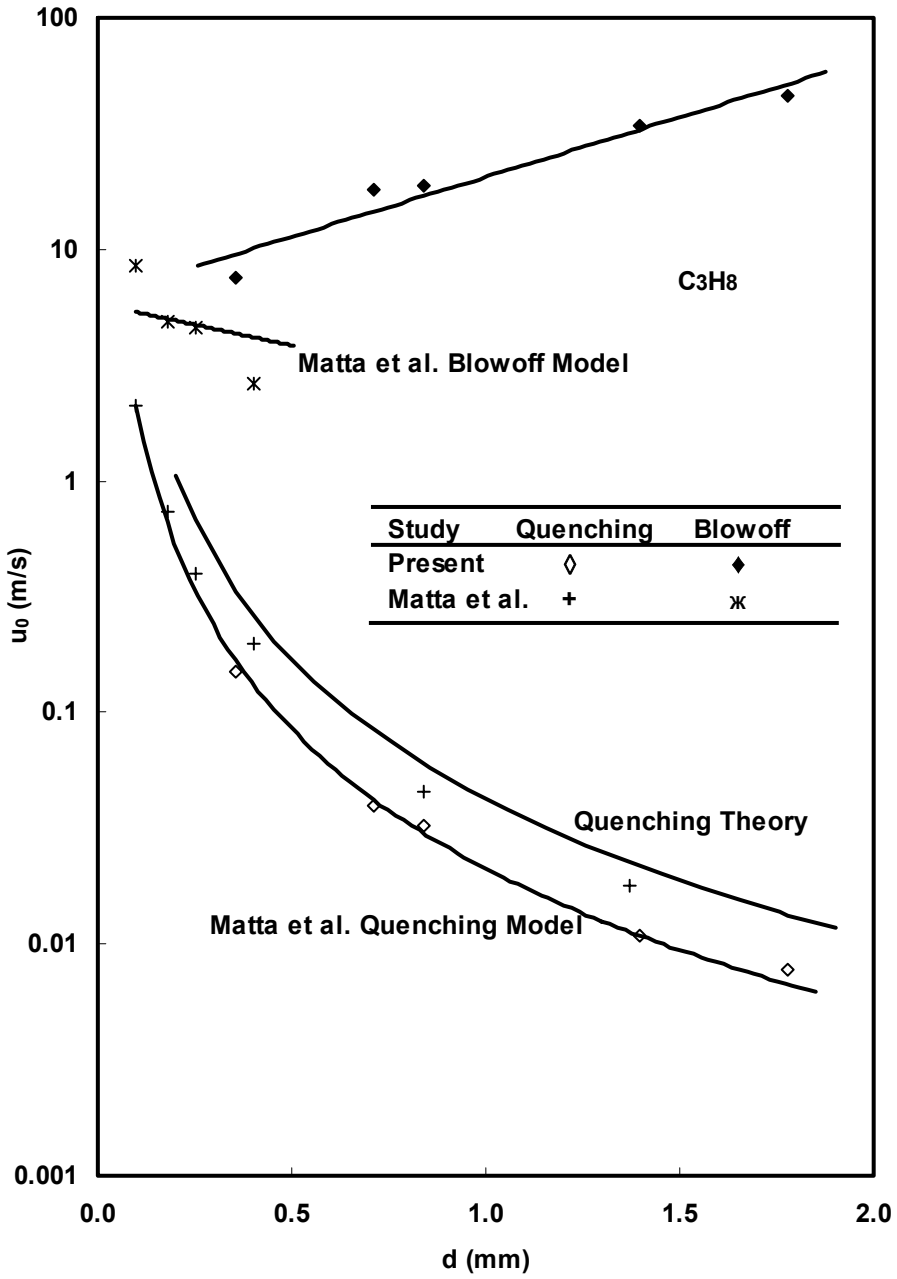

Figure 3.8: Propane quenching and blowoff shown as fuel velocity "u_0" vs. burner diameter. The Quenching Theory line represents the prediction for quenching from the application of Eq. 3.5. The line through the blowoff points is a curve-fit highlighting the trend observed for that phenomenon. Quenching data and model prediction, as well as blowoff data and model prediction for propane from Matta et al. [22] are also shown.

Figures 3.6-3.8 show the quenching and blowoff measurements as fuel velocities versus burner diameter. Data from Matta et al. [22] and Cheng et al. [24] is also included. These figures can help evaluate whether there exists a regime where the flow is either below the quenching limit or above the blowoff limit, for all flowrates possible through a small burner, a theory proposed by [22]. The blowoff limit for hydrogen is so high that it is unlikely such a regime exists. The critical point would be where the blowoff and quench lines cross in Fig. 3.6. This does not appear likely for any burner diameter. As the diameter of the burner falls below a critical diameter, the flow should transition from the continuum flow to a diffusion process, changing the size of the leak in a way that is not reflected in Figs. 3.3-3.8. For flows below a certain critical level, ignition is only possible if confinement causes fuel accumulation, and in that case, quenching is immediate upon the consumption of the accumulated fuel. The consequences and mechanisms of accumulation are beyond the scope of this investigation.

The quenching experiment was also conducted for different burner orientations. The hypothesis is that changing the orientation alters the heat transfer from the flame to the burner, which could cause a change in the quenching limit. Table 3.4 shows the change in flowrate if the burner is rotated vertically 180˚.

Table 3.4: Percentage change in fuel flowrate for inverted cases.

Burner Designation	Hydrogen	Methane	Propane
WN14	0.00	-22.18	58.43
WN28	3.91	-7.04	101.08
WN33	0.63	-7.33	93.46
WN55	7.67	-7.03	84.85
WN70	9.24	-6.52	41.74

Ultimately, no pattern could be identified regarding the influence of burner orientation on the quenching limit. The effect varied by fuel and specific burner. For hydrogen, the impact of orientation was less than a 10% difference in the quenching limit in all instances. Since the focus of the research was hydrogen, and the effect is small for hydrogen, orientation is considered to be non-critical for the discussion of the risks associated with a hydrogen leak.

Chapter 4: Corrosive Effects of Flames

In addition to establishing the conditions necessary to sustain a hydrogen flame, an investigation into the effects of prolonged exposure to hydrogen flames on materials was desired. Myriad examples in the literature are provided indicating that hydrogen exposure at room temperature can have a significant effect on materials, especially metal alloys [18,19,20]. However, little is known about materials degradation associated with impinging hydrogen diffusion flames.

The effects of exposure to hydrogen flames were investigated. The first experiments involved observing the effects on 304 stainless steel tube burners, one supporting a hydrogen flame, the other a methane flame. The final state of the burners is qualitatively assessed. The second series of experiments involved exposing samples of wire and fiber to a hydrogen and a methane flame for different time intervals, and observing any degradation of the wire or fiber material.

4.1 Burner Tube Test

Long term tests were conducted to determine the effects on stainless steel of exposure to a hydrogen and methane flames. These tests involved the use of identical round tubes constructed from 6.35 mm outside diameter 304 stainless steel tubing with 0.318 mm wall thickness.

The flow system setup for these experiments is identical to that used for quenching and blowoff (details in Chapter 3), flame lengths were held constant at 15 mm in length for the duration of the experiment. The camera lens used was a

Nikkor 60mm focal length f/2.8 D lens by Nikon. An ISO 1600 setting was used with a direct sunlight white balance.

The experiments were conducted during a 355 hour continuous burn. The flames burned continuously except for a few minutes each day while images were recorded, and are visible here in Fig. 4.1. Figure 4.2 shows the burners in their pre-test condition. Figure 4.3 shows the burners at the end of the test.

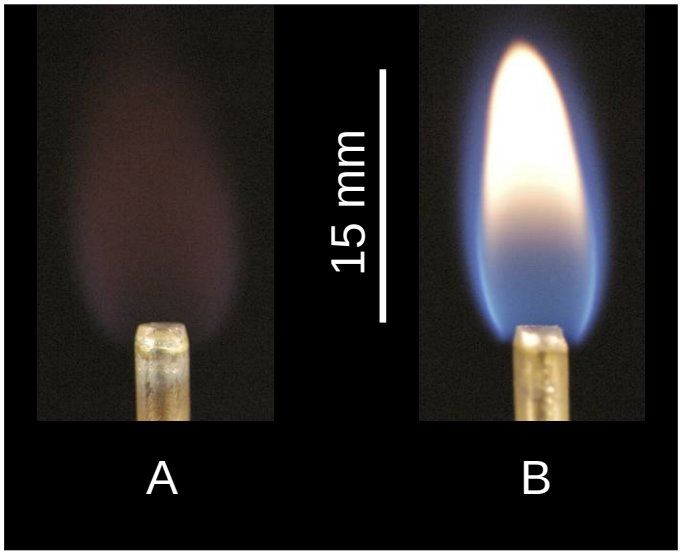

Figure 4.1: Color image of Hydrogen flame and burner (A), Methane flame and burner (B). Camera settings for this shot were ISO 1600, 1/20 sec shutter speed, and f# =3.8.

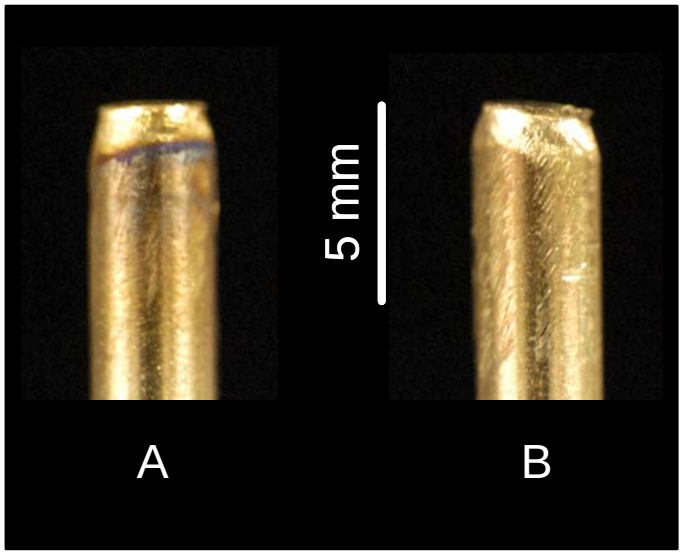

Figure 4.2: Color image of stainless steel tube burners before the long term test. Burner A will be used for hydrogen, while B will be used for methane.

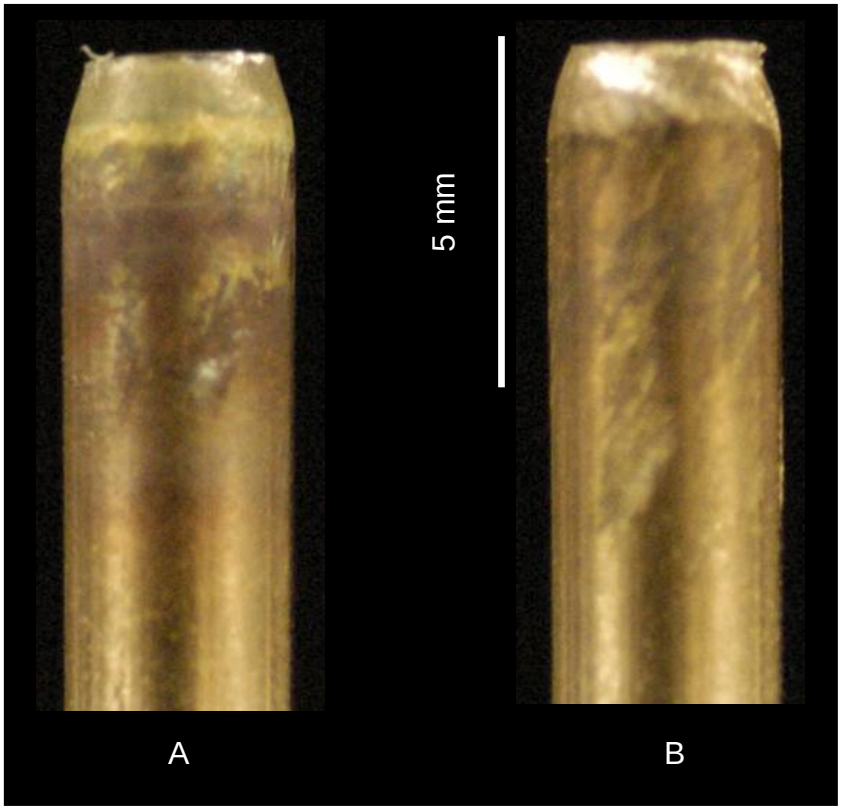

Figure 4.3: Color image of burner A exposed to a hydrogen flame and burner B exposed to a methane flame, each for 355 hours.

At the end of the test, there is a noticeable ring of corrosion on the hydrogen burner, A in Fig. 4.3. This ring was first observed developing after 30 hours, and continued to grow for the duration of the experiment. The ring is located at the position where the hydrogen flame anchored to the burner, as can be seen in Fig. 4.1. This corrosion is either caused by a normal oxidation process, accelerated by the enhanced heating of the burner holding the hydrogen, or it is some other effect related to the concentration of free hydrogen radicals, or a combination of several of these effects. It is related to the fuel, a fact supported by the lack of similar corrosion on the methane burner, but the exact mechanism has yet to be determined.

4.2 Wire and Fiber Experiments

Wire and fiber samples of various materials were suspended in hydrogen and methane flames. By using small sample diameters, 1.0-1.15 mm, the increase in temperature experienced by the material can be increased compared to the long term experiment outlined in Section 4.3.1, exaggerating whatever corrosion is taking place. This accelerated the testing. Table 4.1 outlines the different materials and sizes used.

Table 4.1: Wire and fiber materials and sizes used for the short term experiments.

Material	Diameter (mm)
304 Stainless Steel	1.04
316 Stainless Steel	1.01
Aluminum Alloy 1100	1.01
Galvanized 1006-1008 Carbon Steel	1.04
Ceramic Grade SiCO fiber	1.14

To ensure a similar exposure condition to each flame, both flames were held at the same length, 25 mm. This corresponds to a flowrate of 2.28 mg/s for hydrogen, and 1.62 mg/s for methane. The wires were positioned at 7 mm above the burner tip, which is just below the soot forming region of the methane flame. The burner inside diameter is 2.43 mm.

The alloy 304 stainless steel has a wide range of applications in the transportation, industrial, and architectural fields, making it an ideal choice for examination here. Specifically, 304 stainless steel was chosen because the composition of this alloy makes it ideally suited to welding and drawing [33]. The interaction of hydrogen flames with the alloy is therefore of critical importance as the utilization of hydrogen in transportation applications increases.

Stainless steel alloy 316 is more corrosion resistant than other austenitic stainless steels, including 304 stainless steel [33]. It is therefore worthwhile to also investigate the effects of hydrogen flames on this alloy, as it is the likely substitute for the 304 stainless steel alloy if there is a corrosion problem with 304 stainless steel exposed to hydrogen.

Aluminum is another common material found in many transportation fuel containment systems. The features of aluminum, like corrosion resistance [33], make it well suited to an investigation of the corrosive effects of exposure to hydrogen flames.

Galvanized steel is steel that has been alloyed with zinc to make it more corrosion resistant. Galvanized steel is a popular choice in applications where steel is desired but will be exposed to corrosive conditions. The galvanization process can be

applied to pre-made steel components [33], and so would be another alternative to consider for use where exposure to a hydrogen flame is a possibility.

Silicon-carbide fibers are increasingly used in fuel storage tanks [34]. Specifically, these composites are discussed in relation to the creation of high pressure storage tanks for hydrogen powered vehicles [16]. The effects of exposure of these fibers to an impinging hydrogen flame is therefore of significant interest. Individual filaments of a silicon carbon fiber are tested, as well as an entire fiber yarn. Details of the fiber provided by the manufacturer are presented in Table 4.2.

Table 4.2: SiCO fiber details.

Properties of NICALON™ Ceramic Grade SiCO fibers [102]

Property	**Value**
Fiber Denier	1800
Density, kg/m^3	2550
Composition, weight % Si:C:O	57:32:12
Filament Diameter, μm	14
Tensile Strength, GPa	3.0
Tensile Modulus, GPa	210
Vol. Resistivity, Ω-cm	1000
Dielectric Constant	9.2
Loss factor	1
CTE, ppm/ °C, 0-900 °C	3.9
Thermal Conductivity, W/m-K	
at 25 °C	2.97
at 500 °C	2.20
Specific Heat, J/g-K	
at 25 °C	0.71
at 500 °C	1.17
Surface Treatment	Polyvinyl Alcohol

The short term test of all of these samples involves a direct impinging flame exposure that lasts 1 hour. The wires and fibers are photographed using a Nikon D100 single-lens reflex digital still camera before and after the test.

Longer tests were performed on some materials, extending the short-term tests to longer times. Eight hours was generally used for these tests. The flame lengths and fuel flow rates were the same as for the short term experiments.

4.3 Wire and Fiber Test Results

The results of the short and long term test on the wire and fiber samples is discussed here. Photographs of the samples are presented illustrating relevant aspects of the experiments, and qualitative assessments of material performance are made.

4.3.1 Stainless Steel Alloy 304

The first material tested was stainless steel, alloy 304. For the duration of the short exposures, there is no significant corrosion of the stainless exposed to either fuel. The stainless did reach much higher temperatures when exposed to hydrogen, shown in Fig. 4.4.

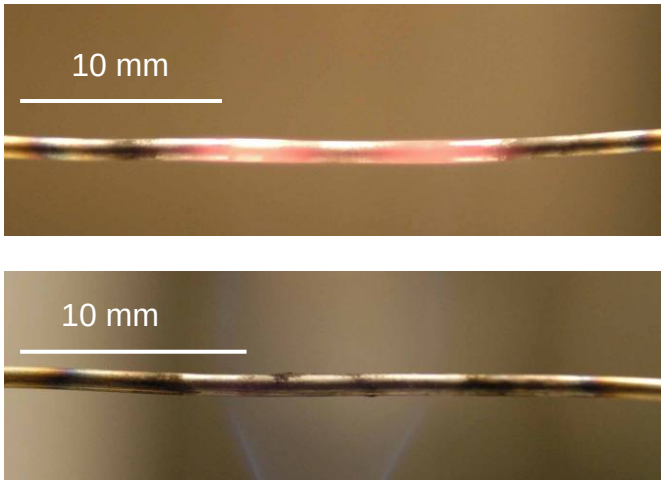

Figure 4.4: Color images of 304 stainless steel subjected to a hydrogen flame (top). The hydrogen flame is invisible under the conditions of the photograph. Stainless steel exposed to a methane flame (bottom).

Prolonged exposure (10 hours) caused some ablative behavior in the stainless steel, shown in Fig. 4.5, at the edges of the glowing region. It is unclear if this material is actually the outer edge of the stainless steel, or if it is a coating that might have been applied in the manufacturing process.

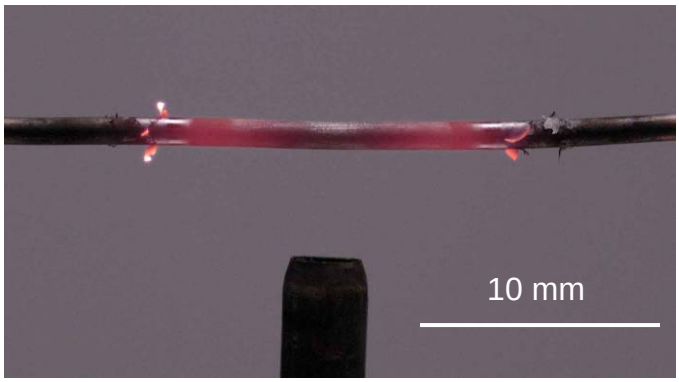

Figure 4.5: Color image of deterioration of the surface of the 304 stainless steel wire is visible after prolonged exposure. A hydrogen flame is present but is not visible here.

According to Metals Handbook [33], this type of wire is often finished using a lead, copper, lime and soap or oxide and soap finish. Irrespective of the presence of a

surfacing material, similar behavior was not evident in an identical piece of wire subjected to methane.

4.3.2 Stainless Steel Alloy 316

Stainless steel alloy 316 was also tested for one hour in both flames. The test showed some staining of the material (Figure 4.6) and some soot deposition, but no visible corrosion, in methane or hydrogen.

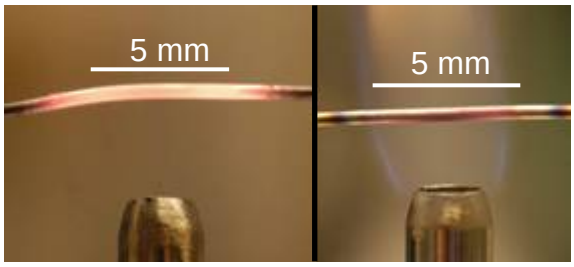

Figure 4.6: Color image of stainless steel alloy 316 exposed to hydrogen (left) and methane (right). The hydrogen flame on the left is evidenced by the glowing wire.

There was no corrosion effect evident after 1 hour of exposure, which demonstrates that alloy 316 has superior corrosion resistance, a claim in [33].

4.3.3 Aluminum Alloy 1100

Aluminum wire subjected to a hydrogen flame for one hour demonstrates visible corrosion and deformation. Shown in Figure 4.7 is the aluminum wire in a hydrogen flame.

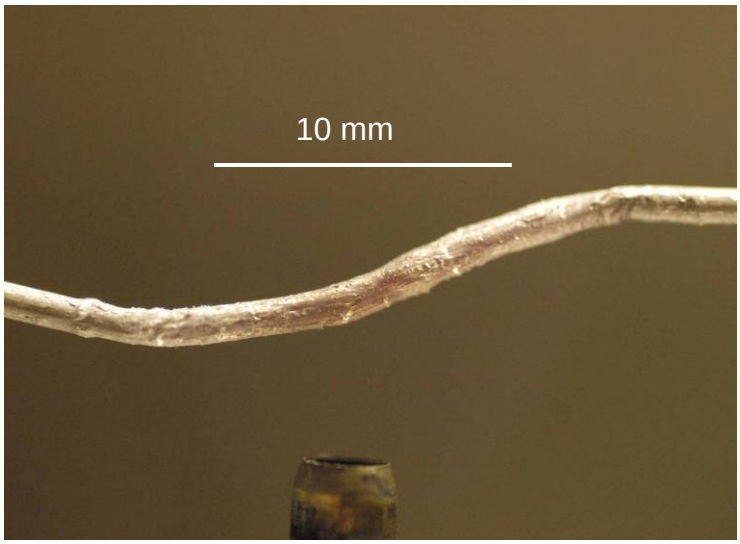

Figure 4.7: Color image of aluminum wire subjected to a hydrogen flame. Corrosion and severe deformation are observed. A hydrogen flame is present in this picture, but not visible.

Increasing the duration of the test to 8 hours, the aluminum wire in the hydrogen flame burns through completely, shown in Figure 4.8.

Figure 4.8: Color image of aluminum wire exposed to a hydrogen flame. This burns completely through (left). Identical exposure duration to a methane flame results in slight visible corrosion and thermal deflection (right).

The result of the 1100 aluminum exposure to a hydrogen flame is a much more rapid breakdown of the material than what was seen with any other material examined.

4.3.4 Galvanized 1006-1008 Carbon Steel

The galvanized carbon steel samples, shown in Figure 4.9, became coated in a yellow residue. However, the residue left on the hydrogen flame sample was outside

the flame region while the residue left on the methane flame was inside the flame region.

Figure 4.9: Galvanized 1006-1008 Carbon steel after 1 hour exposure to hydrogen (left) and methane (right). The scale markings are in mm. No flames are present.

The residue on the hydrogen flame sample was more concentrated and thicker than the methane flame sample. The hydrogen flame sample also showed some degradation, mostly within the flame region. These samples did not have the typical discoloration that was found on most of the other samples.

4.3.5 SiCO Fiber

Filaments in the hydrogen and methane flames were observed to fail in 15 and 116 minutes, respectively. The two fibers in the flame can be seen in Figure 4.10.

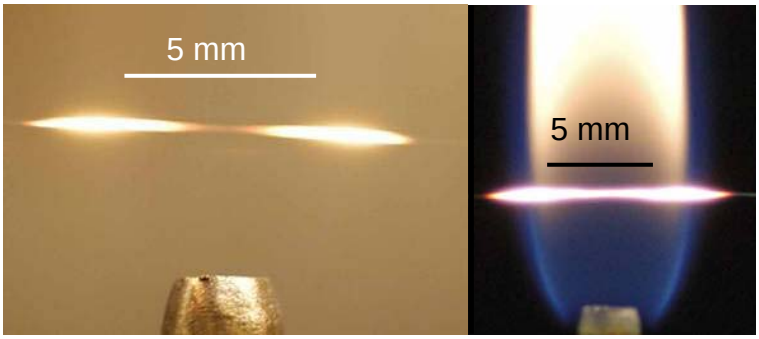

Figure 4.10: Color image of carbon fiber in hydrogen flame (left), carbon fiber in methane flame (right).

A single strand fiber is not especially indicative of the SiCO fiber performance, and the extremely small diameter relative to the other wires (14 μm vs. 1.01 mm) tested also complicates a comparison of carbon fiber to those materials based on this one hour test. A yarn of carbon fiber (1.14 mm) was therefore tested for

one hour. Loose strands on the exterior of the fiber in hydrogen burned through (one or two individual fibers), but the larger portion of the fibers remained intact. The yarn can be seen in the hydrogen flame in Figure 4.11.

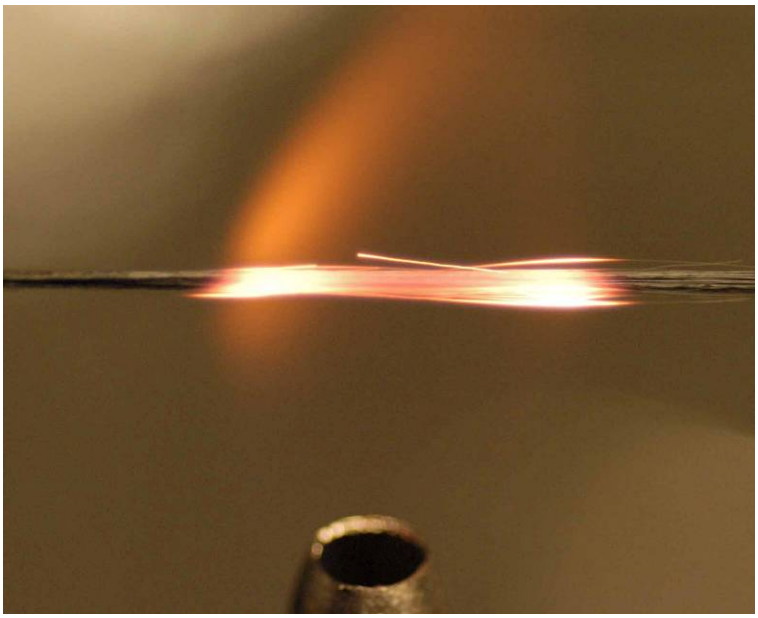

Figure 4.11: Color image of carbon fiber yarn and hydrogen flame after one hour.

The yarn was then exposed to a longer exposure to both flames. After 13 hours, five individual strands burn through on the yarn in the hydrogen. Two fibers from the yarn exposed to methane burn through as well. In both cases the bulk of the fibers remain intact after prolonged exposure. The two samples following this test are shown in Figure 4.12.

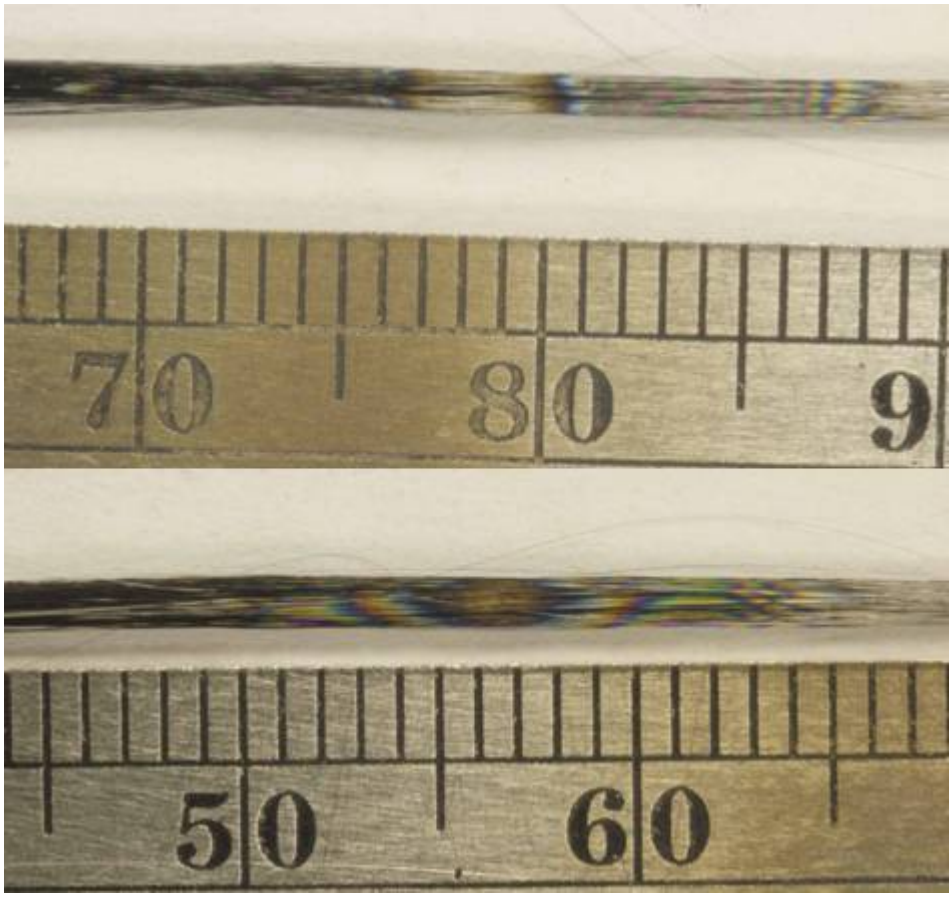

Figure 4.12: Color image of carbon fiber yarn exposed to hydrogen (top) and similar sample exposed to methane (bottom). Fibers that broke during the experiment are visible faintly above each sample. The scale shown is mm. No flames are present.

The difference in performance between the two yarn samples is not significantly different. The tight bundle of fibers that comprises the bulk of the material remained intact after 13 hours.

Chapter 5: Conclusions

Quenching and blowoff limits were measured experimentally. A model for quenching phenomena was also derived and presented as a dimensionless crack parameter. Materials degradation effects caused by exposure to hydrogen and methane flames were investigated. The major conclusions drawn from these research efforts are presented here.

5.1 Quenching and Blowoff

The quenching and blowoff limits for hydrogen, methane, and propane have been modeled and measured for small round burners. The fuel mass flow rate at the quenching limit was found to be independent of burner diameter. Quenching limits for hydrogen were found to be lower than those for propane and methane. The average quenching flowrate for hydrogen through stainless steel burners was found to be 0.022 mg/s. The theoretical prediction for quenching captured the trends and curves of the data, but actual values based on the premixed quenching distances were not very accurate. Quenching limits for propane and methane agree with those measured by Refs. [22,24].

Blowoff flowrates for hydrogen, methane, and propane, were found to be sufficiently large to counter the hypothesis that there might be a regime where a leak was either too small to support a flame, or too fast to prevent blowoff. Hydrogen has significantly higher flowrates at blowoff than methane or propane, likely due to the much higher laminar burning velocity of hydrogen.

5.2 Materials Effects

Aluminum alloy 1100 experienced much higher corrosion in the hydrogen flame than any steel tested. Complete failure of the aluminum wire was observed after 8 hours. Consequently, aluminum is not well suited applications involving exposure to hydrogen flame.

Stainless Steel alloy 304 suffered some slight corrosion effects when exposed to the hydrogen flame. Alloy 316 performed better than 304, experiencing less corrosion for the same exposure time. Either alloy is probably adequate for use around hydrogen flames, but 316 is better suited than 304.

Galvanized carbon steel experienced some slight corrosion in the hydrogen flame, as the layer of galvanization ablated. A yellow residue was deposited on the galvanized carbon steel wire exposed to either flame, this deposition was located within the flame region for the methane sample, and outside the flame region on the hydrogen sample.

Ceramic grade SiCO fibers performed similarly for hydrogen and methane exposure. Individual fibers are broken during the exposure, fibers in hydrogen breaking faster than those in methane. Yarn comprised of many of these fibers performed well. This material is probably well suited for use where exposure to hydrogen flames is possible.

Bibliography

[1] Schrope, M., Which Way to Energy Utopia?, Nature 414 p 682-684, (2001).

[2] Morton, N.R., Sunderland, P.B., Chao, B.H., Axelbaum, R.L., Fire Hazards and Materials Degradation Effects of Small Hydrogen Leaks. Conference Paper, San Diego (2007).

[3] Morton, N.R., Sunderland, P.B., Chao, B.H., Axelbaum, R.L., Fire Hazards of Small Hydrogen Leaks. Conference Paper, SAE World Congress. Detroit (2007).

[4] Morton, N.R., Sunderland, P.B., Chao, B.H., Axelbaum, R.L., Fire Safety Risks Associated with Leaks in Hydrogen Systems. Poster, Annual Fire Conference, National Institute of Standards and Technology, Gaithersburg (2006).

[5] Morton N.R., Sunderland, P.B., Chao, B.H., Axelbaum, R.L., Fire Hazards of Small Hydrogen Leaks. Poster, Bridging the Transition...Hydrogen Internal Combustion Engines Symposium, weststart.org, San Diego (2006).

[6] Sato, Shinya., Lin, Shi-Ying., Suzuki, Yoshizo., Hatano, Hiroyuki., Hydrogen Production from Heavy Oil in the Presence of Calcium Hydroxide. National Institute of Advanced Industrial Science and Technology, Institute for Energy Utilization, 305-8569, Japan 2002.

[7] Bregeon, Bernard., Gordon, Alvin S., and Williams, Forman A., Near-Limit Downward Propagation of Hydrogen and Methane Flames in Oxygen-Nitrogen Mixtures. Combustion and Flame 33:33-45, (1978).

[8] Turns, Stephen R., An Introduction to Combustion. McGraw-Hill, (2000).

[9] Bove, R., Lungh, Px, Allessio, L., Sames, N.M., Biogas as Fuel for a Fuel Cell System: Investigations and First Experimental Results for a Molten Carbonate Fuel Cell. Journal of Fuel Cell Science and Technology ASME. 1: 21-24.

[10] Lovins, A.B. Twenty Hydrogen Myths, Final Report. Rocky Mountain Institute Snowmass, CO, 2003.

[11] Pickard, P.S., Material Challenges for Hydrogen Production from Nuclear Systems., Transactions of the American Nuclear Society: Nuclear Fuels and Structural Materials for the Next Generation Nuclear Reactors v. 94. p. 693 (2006).

[12] Lee, I.D., Smith, O.I., Karagozian, A.R., Hydrogen and Helium Leak Rates from Micromachined Orifices. AIAA J. Vol. 41, No. 3, p. 457-464 (2003).

[13] Bossel, U.B., Eliasson, B. The Future of the Hydrogen Economy: Bright or Bleak?. Proc. Of Fuel Cells World, Lucerne, Switzerland, July 2002.

[14] Cadwallader, L.C. and Herring, J.S., Safety Issues with Hydrogen as a Vehicle Fuel, Report INEEL/EXT-99-00522, prepared for U.S. Department of Energy (1999).

[15] Khan, R., Kan, Z., Al-Sulaiman F., Merah, N., Fatigue Life Estimates in Woven Carbon Fabric/Epoxy Composites at Non-Ambient Temperatures. Journal of Composite Materials Vol. 36, No. 22, p. 2517-2535 (2002).

[16] Young, K.S., Hydrogen Storage Alternatives – A Technological and Economic Assessment. International Journal of Hydrogen Energy v 17, n 7, p 505-507 (1992).

[17] Pehr, K. Aspects of Safety and Acceptance of LH2 Tank Systems in Passenger Cars. Int. J. Hydrogen Energy Vol. 21, No. 5, pp. 387-395 (2006).

[18] Utgikar, V.P., Thiesen, T., Safety of compressed hydrogen fuel tanks: Leakage from stationary vehicles. Technology in Society 27:315-320 (2005).

[19] Dayal, R.K., Hydrogen permeability and its relation to embrittlement effect in various materials. Trans Indian Inst Met 56:319-326 (2003).

[20] Mallikarjun MM. Materials of construction for hydrogen service. Chem Age India 23:368-72, (1972).

[21] Swain, M.R., Swain, M.N., A Comparison of H2, CH4, and C3H8 Fuel Leakage in Residential Settings, Int. J Hydrogen Energy 17:807-815 (1992).

[22] Matta, L.M., Neumeier, Y., Lemon, B., Zinn, B.T., Characteristics of Microscale Diffusion Flames. Proceedings of the Combustion Institute v. 29. n.1, p 933-938 (2002).

[23] Lee, B.J., Cha, M.S., Chung, S.H., Characteristics of Laminar Lifted Flames in a Partially Premixed Jet. Combustion Science and Technology Vol. 127, pp. 55-70 (1997).

[24] Cheng, T.S., Chen, C.P., Chen, C.S., Li, Y.H., Wu, C.Y., Chao, Y.C., Characteristics of Microjet Methane Diffusion Flames. Combustion Theory and Modeling v.10, n. 5, p. 861-881 (2006).

[25] Vanquickenborne, L.,van Tiggelen, A., The stabilization Mechanism of Lifted Diffusion Flames. Combustion Flame 10: 59-69 (1966).

[26] Seade, J.P., Chen, L.D., Roquemore, W.M., Liftoff Characteristics of Methane Jet Diffusion Flames. Journal of Propulsion and Power v. 9. n. 4, p. 654-656 (1993).

[27] Peters, N., Williams, F.A., Liftoff Characteristics of Turbulent Jet Diffusion Flames. AIAA J. 21: 423-429 (1983).

[28] Rizk, N.K., Lefebvre, A.H., Influence of Laminar Flame Speed on the Blowoff Velocity of Bluff-Body-Stabilized Flames. AIAA J. v. 22, n. 10, p 1444-1447 (1984).

[29] Kanury, A.M., Introduction to Combustion Phenomena. Gordon and Breach, New York, p. 131 (1975).

[30] Ezekoye, O.A., Heat Transfer Consequences of Condensation during Premixed Flame Quenching. Combustion and Flame 112:266-269 (1998).

[31] Roper, F.G., The Prediction of Laminar Jet Diffusion Flame Sizes: Part I. Theoretical Model. Combust. Flame 29:219-226 (1977).

[32] Sunderland, P.B., Mendelson, B.J., Yuan, Z.-G., Urban, D.L., Shapes of Buoyant and Nonbuoyant Laminar Jet Diffusion Flames. Combust. Flame 116:376-386 (1999).

[33] Metals Handbook. Properties and Selection. Ninth Edition, prepared by American Society for Metals. Volume 1-3. Metals Park, Ohio, 1983.

[34] Cohen, D., Composites - Part A: Applied Science and Manufacturing, v 28, n 12, p 1035-1047 (1997).